Int. Journ. of Fracture 21 (1983) 163-176. 0376-9429/83/03/0163-14$0.20



# Crack extension caused by internal gas pressure compared with extension caused by tensile stress*

STUART McHUGH**

*Shock Physics and Geophysics Department, Poulter Laboratory, SRI International, Menlo Park, CA 94025, USA*

(Received December 19, 1980; in revised from December 15, 1981)

ABSTRACT

Explosive loading in borehole configurations has been investigated to assess the relative importance of internal gas pressurization and stress-wave-induced circumferential tensions for extending radial cracks originating at the borehole walls. Simple calculations of an extending crack (with and without confining pressure) were performed to estimate an upper bound on crack length resulting solely from internal pressurization for comparison with the crack length resulting solely from tensile stresses. These calculations indicated that a internal gas pressure could increase the crack length by a factor of 10 to 100 (no confining pressure) or 3 to 25 [6.9-MPa (1000-psi) confining pressure] compared with the tensile stresses acting alone. Simple laboratory experiments were performed using $3.2 \times 10^{-3}$ m diameter (1/8 in.) by $1.52 \times 10^{-1}$ m long (6 in.) borehole charges centered in a $1.3 \times 10^{-2}$ m diameter (1/2 in.) borehole in transparent Plexiglas cylinders $3 \times 10^{-1}$ m in diameter by $3 \times 10^{-1}$ m long (12 in. by 12 in.) to verify these computational results. Two tests were performed: one with a thin ($5.08 \times 10^{-4}$ m) steel liner to contain the explosive gases and one without a liner so that the explosive gases could enter and pressurize the fractures. A confining pressure of 6.9 MPa (1000 psi) was applied to the Plexiglas cylinders in both experiments to better simulate field conditions and to contain the cracks within the cylinder; all other experimental conditions were identical. These experiments indicated that the primary effect of the explosive gases was to increase crack length by a factor of five to ten compared with the tensile stresses acting alone, in approximate agreement with the predictions.

## 1. Introduction

Although the use of explosives to fracture and rubblize geologic materials is a well-established technique [1, 2] and is extensively used to recover a variety of natural resources, it is difficult to characterize the fracture phenomenology and computationally simulate fracture initiation, growth, and coalescence. This, in turn, makes it difficult to design optimum explosive-loading procedures. In this paper, the experimental and theoretical effects on fracturing produced by internal pressurization of crack surfaces and tensile stresses are compared with the effects produced by tensile stresses alone in a dynamic, laboratory-scale borehole shooting configuration.

Field and laboratory experiments, discussed in more detail below, suggest that the following sequence of events occurs in a dynamic borehole shot. As the explosive (or propellant) releases its energy, stress waves propagate into the material. When the circumferential stresses become tensile, radial cracks nucleate and grow. Typically, several of these cracks may intersect the borehole. If these cracks are open, the explosive detonation products (gases) can enter the cracks, pressurize the internal crack surfaces, and contribute to crack growth. If the cracks are not open to the gases (e.g., because the borehole is sheathed or the cracks are clogged with debris), only the tensile stress waves will cause crack extension. Therefore, the effect on crack extension of the gas pressure within the cracks must be distinguished from the

* This work was partially sponsored by the Department of Energy, Morgantown Energy Technology Center, Morgantown, WV, under Contract No. DE-AC21-79-MC11577.

** Now at Lockheed Missile and Space Co., Bldg. 204, 3251 Hanover St., Palo Alto, Ca. 94304 USA.

effect of tensile stresses acting alone if we are to design optimum explosive-loading procedures.

Previous theoretical and computational studies [3–16] have investigated (1) the effects of an internal pressure on crack instability; (2) the role of borehole pressure, internal pressure, and crack length in the stability criterion for a system of several radial fractures extending from the borehole; and (3) the interaction of the fluid pressure within the crack and the borehole pressure. Experimental work by Kutter and Fairhurst [17] and Porter and Fairhurst [18] was performed assuming that the shock wave fractured the material around the borehole and that the subsequent gas pressure was quasi-statically exerted against the walls of this highly fractured cavity. A quasi-static pressurization, however, causes only one or two fractures to extend rather than the five to ten typically observed in dynamic borehole shooting configurations [2, 19].

Dally *et al.* [20] experimentally examined the effect of gas pressure from an explosive charge that fractured a $6.4 \times 10^{-3}$ m thick (0.25 in.) plastic sheet. However, in one test the charge was contained, and in the second the charge vented. Hence the stress histories (e.g., peak pressures and durations) at the borehole wall in the two experiments were probably substantially different, and thus separating the roles of the shock wave and gas pressure in the fracture process was difficult.

Field experiments by Coursen [21] and Warpinski *et al.* [19] using explosives or propellants demonstrated that in borehole shooting the detonation/deflagration products could enter fractures and probably cause crack extension. However, the role of the shock-wave-induced stresses was not analyzed in these experiments because the observed crack lengths could be reproduced assuming that the internal gas pressurization effects predominated.

In the following discussion the effects of the tensile stresses acting alone to produce fracturing are determined; then the effects of an internal gas pressure on fractures are modeled and compared with the tensile stress effects. The borehole shooting experiments described later are quite complex; that is, several radial fractures of different lengths are linked to the borehole and propagate under the combined effect of the dynamic tensile stress and an internal gas pressure (and both the tensile stress and gas pressure and their gradients change with time). Because of this complexity, only the primary aspects of fracturing are considered and simple models are used to analyze fracturing for the conditions of interest and to establish bounds on the fractures lengths.

## 2. Fracturing caused solely by dynamically applied tensile stress

Before the problem of crack extension by internal pressurization is considered, it is instructive to examine the extent of fracturing that might be expected from the dynamic tensile stress alone for a typical, dynamic, laboratory springing (i.e., cylindrical borehole) experiment. Then crack lengths derived from an analysis of internal pressurization (i.e., on the crack faces) can be compared with the crack lengths resulting from dynamically applied tensile stresses to evaluate the importance of the gas pressure effects.

SRI's NAG-FRAG [22] computational subroutine was developed to model crack nucleation by tensile stresses, crack growth by combined tensile stresses and internal gas pressurization, and crack coalescence. The NAG-FRAG model does not treat individual cracks, but rather deals with populations of crack arrays. The NAG-FRAG model uses empirically derived nucleation, growth, and coalescence parameters to predict the number density (number per unit volume) of cracks, crack size distributions and orientation, void

volume, and the fragment size distribution. The NAG-FRAG computational subroutine was used in the PUFF [23] one-dimensional wave propagation code to simulate fracture in a cylindrical geometry for the experiments described in Section 4. Details of similar simulations are in Refs. [24] and [25].

In the NAG-FRAG calculational simulations of fracturing in the experiments described in Section 4, it was assumed that the tensile stresses acted alone and that a 6.9-MPa (1000-psi) confining pressure was applied. Because the tensile stresses control fracture nucleation and growth in the model, the calculated fracture zone for these laboratory springing experiments primarily consists of radial fractures caused by the circumferential tensile stresses. The simulations indicated that the maximum extent of the several fractures would be 0.02 to 0.05 m, corresponding to a fracture threshold stress of 25 MPa and 10 MPa, respectively. That is, 0.02 to 0.05 m is approximately the extent of the region around the borehole within which the circumferential tensile stress is greater than the fracture threshold stress.

To compare these results with fracturing under other conditions, we performed calculational simulations of fracturing in similar laboratory borehole shooting experiments in other materials (e.g., shale) but with zero confining pressure. These simulations indicated that the maximum extent of the cracks would be $5 \times 10^{-3}$ to $1.5 \times 10^{-1}$ m, depending on the input stress pulse [24].

These results suggest that the shock wave and the dynamic hoop tensions from the detonation of a cylindrical column of explosive in typical laboratory borehole shooting experiments and confining pressures of 0 to 6.9 MPa (1000 psi) may produce several fractures from $5 \times 10^{-3}$ to about $1.5 \times 10^{-1}$ m in radius [25].

## 3. A model for crack extension due solely to internal gas pressurization

In an actual, dynamic, laboratory springing experiment, the crack growth is the result of the growth caused by the shock-wave-induced tensions and the growth caused by the explosive detonation products infiltrating the cracks and internally pressurizing the crack surfaces. However, the results of some field and laboratory experiments have suggested that internal gas pressurization effects may predominate over the effect of the tensile stresses [1, 19, 21]. Consequently, in the following discussion it is assumed that the effect of an internal gas pressure can be examined separately from the effect of tensile stresses.

To examine the role of the explosive gases in more detail and especially to determine whether the gas pressure in the borehole could produce sufficient pressure in the crack to cause extension, we developed a model of an expanding crack for use in computational simulations of gas flow. As the explosive detonates, the pressure rise in the borehole is caused by the shock wave generated by the explosive plasma and the evolution of the gaseous detonation products. To examine whether gas flow alone from borehole to crack is sufficient to cause crack growth, the transient borehole pressure pulse is not treated here. In the model it was assumed that the expanding crack (connected to the borehole and without any confining pressure applied) could be represented as shown in Fig. 1. Here the borehole is treated as a reservoir of gas (at an initial pressure of $P_1^0$ and a constant volume of $v_1^0$), and the crack is an expanding chamber with pressure and volume $P_2(t)$ and $v_2(t)$.

The GASLEAK code [26] (originally developed for expanding piston problems) was used to compute the mass flux from Chamber 1 to Chamber 2 using the procedure diagrammed in Fig. 2. The radius of the "crack" was allowed to extend at a constant growth velocity, $V_g$, whenever the stress intensity, $K_I$, at the "crack tip" exceeded the fracture toughness, $K_{Ic}$, of the material. Here $K_{Ic}$ is assumed to be 1.1 MPa$\sqrt{\text{m}}$ (1 ksi$\sqrt{\text{in.}}$), which is

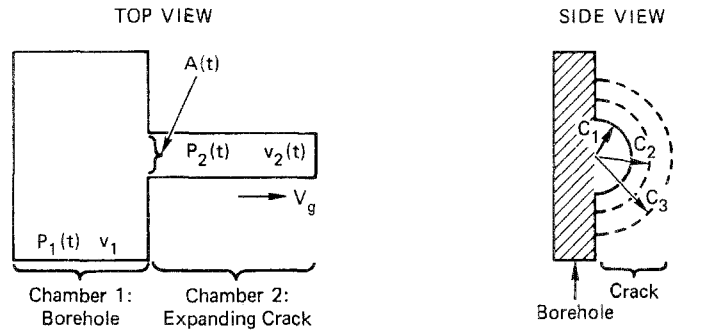


| | | |
|---|---|---|
| $P_1^\circ$, $v_1^\circ$ | = | Initial borehole pressure and volume |
| $P_2(t)$, $v_2(t)$ | = | Pressure and volume in the expanding crack |
| $A(t)$ | = | "Orifice" area; area of intersection of crack with borehole |
| $V_g$ | = | Crack extension velocity |
| $C(t)$ | = | Crack radius ($C_1$, $C_2$, $C_3$ are radii at different times) |

Figure 1. A model for determining the gas pressure in an expanding crack.

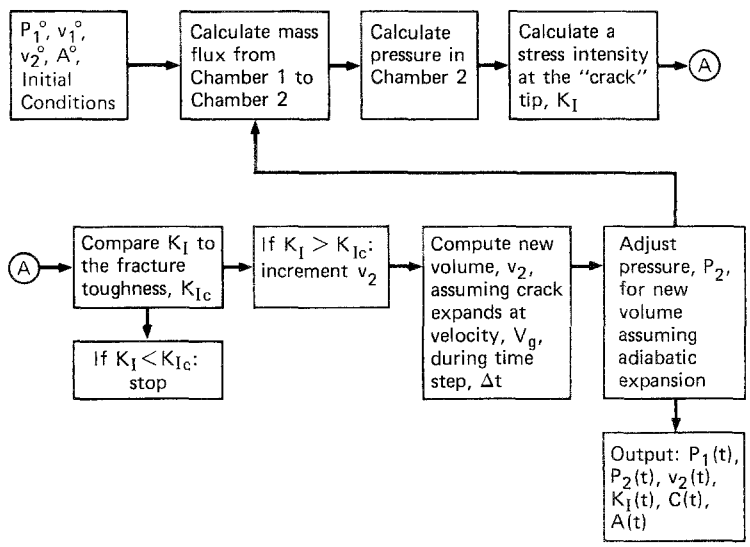


Figure 2. Sequence of events to determine the pressure in the expanding crack. Notation is given in Fig. 1.

representative of some shales and also Plexiglas [25]. No distinction was made in these simple calculations between fracture and arrest toughnesses; that is, $K_{Ia}$ was assumed to equal $K_{Ic}$. The stress intensity at each time step was the product of the pressure in the crack, $P_2$ and the square root of the crack radius, $\sqrt{C}$. (In general, $P_2\sqrt{C}$ would have to be multiplied by a numerical coefficient that depends on crack shape and the existence of a pressure gradient in the crack. Although the coefficient affects the final crack length, it does not alter the modelling procedure discussed here.)

The results of one GASLEAK simulation of an expanding crack are shown in Figs. 3 and 4. The initial conditions ($P_1^0 = 500$ MPa, $v_1^0 = 8.04 \times 10^{-6}$ m$^3$) were specified for a laboratory springing experiment without confining pressure [25], and the crack volume $v_2$ was computed assuming a half-penny-shaped crack. Although the details of the simulation vary

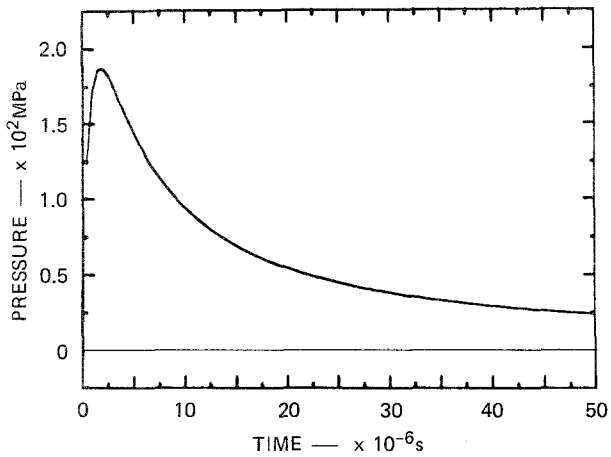


Figure 3. Pressure in the crack *versus* time.

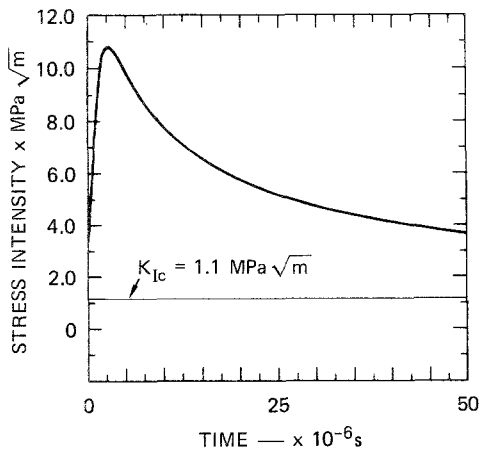


Figure 4. Stress intensity at crack tip.

depending on the assumptions made for the initial conditions and crack shape, these calculations show that (1) significant internal pressures can occur within an expanding crack and (2) the stress intensity at the crack tip can exceed the fracture toughness long enough for the crack to grow to distances significantly greater than the crack lengths produced by the tensile stresses alone.

These calculations also suggested that an upper bound on the final crack length of a half-penny-shaped crack extending from a borehole could be estimated when gas penetration effects predominate. This can be done by neglecting the shock wave-induced tensile stresses and relating the stress intensity stability criterion to the decrease in the borehole and internal crack pressures caused by the increase of crack volume. This approach is developed in detail in the Appendix. From the results in the Appendix we have

$$C^{2-[1/(2\gamma)]} + \left(\frac{2v_i}{\pi nw}\right) C^{-[1/(2\gamma)]} - \left(\frac{2v_i}{\pi nw}\right)\left[\frac{2}{\sqrt{\pi}}\frac{P_i}{K_{Ia}}\right]^{1/\gamma} = 0, \tag{1}$$

where the initial borehole pressure and volume (i.e., before crack growth) are $P_i$ and $v_i$

respectively, the final crack length is $C$, the number of cracks is $n$, the crack width is $w$, the ratio of specific heats of the gas is $\gamma$, and the fracture arrest toughness is $K_{1a}$. Although Eqn. (1) was derived for a condition of no confining pressure, the same method can be used when a confining pressure is applied as described in the Appendix. [However, the resulting (A-16) was not solved analytically.]

For typical laboratory springing experiments without confining pressure, (1) has the approximate solution of

$$C \sim \left(\frac{2v_i}{n\pi w}\right)^{\left(\frac{2\gamma}{4\gamma-1}\right)} \left[\frac{2P_i}{\sqrt{\pi}K_{1a}}\right]^{\left(\frac{1}{2\gamma-0.5}\right)} \tag{2}$$

Equation (2) is plotted in Fig. A-3 in the Appendix for different initial pressures $P_i$, for 1, 5, and 10 cracks, and for a typical laboratory springing experiment. Also shown in Fig. A-3 are the crack lengths for the same initial conditions with a 6.9-MPa (1000-psi) confining pressure applied. Applying a 6.9 MPa confining pressure reduces the crack length by a factor of 2 to 3.

Comparing the crack lengths derived from (2) with the crack lengths expected for the case of tensile stresses acting alone (Section 1) shows that the internal gas pressure may result in cracks 10 to 100 times longer than the cracks extended solely by tensile stress if no confining pressure is applied. Figure A-3 also shows that for a 6.9-MPa confining pressure and the laboratory experiments described in Section 4 (with $P_i \sim 100$ MPa) the crack lengths for internally pressurized cracks are 3 to 25 times longer than those for the tensile stresses acting alone (i.e., 0.15 to 0.50 m* compared with 0.02 to 0.05 m).

Implicit in this analysis are the assumptions that (1) the cracks can be treated independently (i.e., stress relaxation effects are neglected) and (2) there are no pressure gradients in the cracks. When the laboratory samples were sectioned or the field experiments were excavated (i.e., mineback), it was found that at least several fractures had grown and that these fractures contained explosive gases (the explosive residue stained the fractures). However, the internal gas pressure was not known. If the explosive gases had acted quasi-statically, only one or two, rather than several, of the fractures would have extended. Because several fractures extended, this suggests that these cracks extended somewhat independently of one another. Significant cooling of the explosive gases, which should occur in very long fractures in field experiments, will cause a pressure gradient in the crack, and other conditions (e.g., surface roughness of the crack faces that might interfere with gas flow) may also cause pressure gradients within the crack. The consequence of a declining pressure gradient within the crack or a confining pressure larger than 6.9 MPa would be to decrease the final crack length compared with the lengths predicted by (2) or (A-16).

## 4. Experiments

To verify the model discussed in the previous sections, we performed two laboratory springing experiments. The experiments were intended to determine whether the explosive gases would penetrate the fractures and thereby significantly pressurize the fractures, and to quantitatively examine the effects of dynamic gas pressurization on the fracture pattern. Previous laboratory springing experiments did not clearly differentiate between the effects of the tensile stresses and the gas pressure, but the techniques for these types of experiments are

* Because the actual fracture volume in the experiments is not precisely known, a range in crack lengths is noted using a lower bound of 0.15 m for 10 cracks extending to an upper bound of 0.50 m for 1 crack extending. This range is quoted for $P_i \sim 100$ MPa, which corresponds to the peak pressure calculated for these experiments.

well established. Therefore, we decided the new phenomenology experiments should model as closely as possible the laboratory experiments previously conducted [24].

Two experiments were performed using cylinders of Plexiglas Type G. (The cracks produced in Plexiglas can be easily observed.) We used a sheathed borehole in one experiment to contain the explosive gases and an unsheathed borehole in the other so that the gases could penetrate the fractures. As in the previous laboratory experiments, a 6.9 MPa–(1000-psi) confining pressure was added to contain the fractures within the cylinders. A steel liner sheathed the borehole boundary.

Because sheathing the borehole also somewhat changes the stress input to the material, computational simulations (referred to in Section 2) of the experiments were performed to determine the stress histories of the material. These simulations of the sheathed and unsheathed borehole experiments indicated that the cracks would be 0.02 to 0.05-m long (for a peak borehole pressure of about 100 MPa) in either experiment if only the circumferential tensile stresses, and not gas pressurization, extended the cracks.

For these phenomenology experiments, the following configuration was used: two Plexiglas cylinders 0.30 m long (12 in.) and 0.30 m in diameter (12 in.) were constructed by cutting pieces from 0.10-m-thick (4 in.) plates. The pieces were glued with an acrylic cement. A 0.013-m-diameter (1/2 in.) borehole was drilled along the axis of each block. The PETN charges were $3.2 \times 10^{-3}$ m diameter (1/8 in.) and $1.52 \times 10^{-1}$ m long (6 in.), centered in the borehole. Preliminary tests demonstrated that a $5 \times 10^{-4}$ m thick (0.020 in.) steel sheath could survive detonation of a charge of PETN and contain the explosive gases, and this sheath was used in the experiments. The borehole needed to be plugged so that the explosive gases would not escape. Therefore we drilled a 0.025 m diameter (1 in.) by 0.013 m deep (1/2 in.) hole into both ends of the borehole. A layer of Silastic was put into the base of the hole, and the

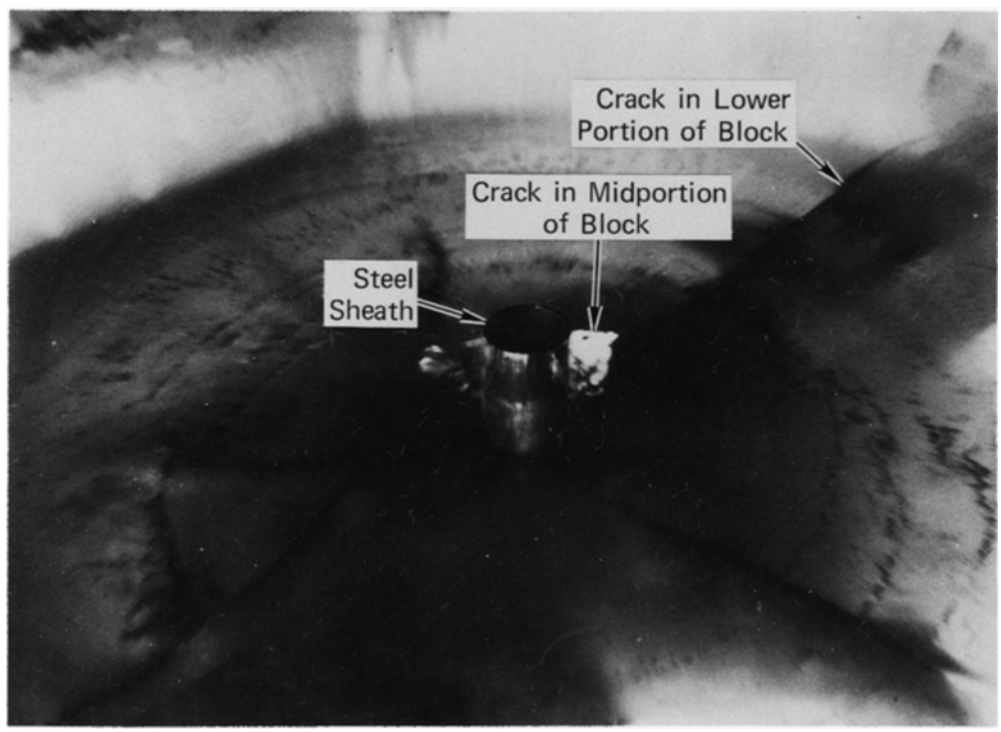


Figure 5. Oblique view of midplane of plexiglas block after detonation of explosive – sheathed borehole.

hole was sealed by gluing a Plexiglas plug into the borehole and a phenolic plug into the 0.025-m-diameter (1 in.) hole. Two borehole pressure gages had also been emplaced at the midplane of the Plexiglas blocks. (However, they failed to operate as intended and will not be discussed further.)

Each Plexiglas cylinder was placed in a pressure vessel, and the confining pressure of 6.9 MPa was applied to contain the cracks within the cylinders. After the charge was detonated, the cylinder was removed from the vessel, sectioned, and photographed.

The cracks produced in the sheathed borehole experiment are shown in Fig. 5. Several features of this test were immediately apparent: the cracks (except near the free surfaces) were vertical, half-penny shaped, and extended radially away from the borehole. The cracks produced in the midsection of the block did not cross the interfaces, i.e., between the 0.10-m-thick sections. The cracks in the midsection were much smaller than those in the lower block, and the cracks in the midsection showed no traces of explosive residue. The cracks in the lower section were heavily stained by the residue. These results showed that the borehole plug failed, allowing the explosive gases to penetrate the cracks in the lower section. However, the cracks in the midsection were apparently affected only by the circumferential tensile stresses.

The cracks produced in the Plexiglas block with no sheath are shown in Fig. 6, and the cumulative number of cracks, $N$, *versus* crack radius, $C$, is compared with the sheathed borehole experiment in Fig. 7. The midportion of the block in the unsheathed experiment contains large half-penny-shaped, vertical cracks that extend radially from the borehole and are darkened by the explosive residue. This darkening indicates that the cracks were internally pressurized by the explosive gases.

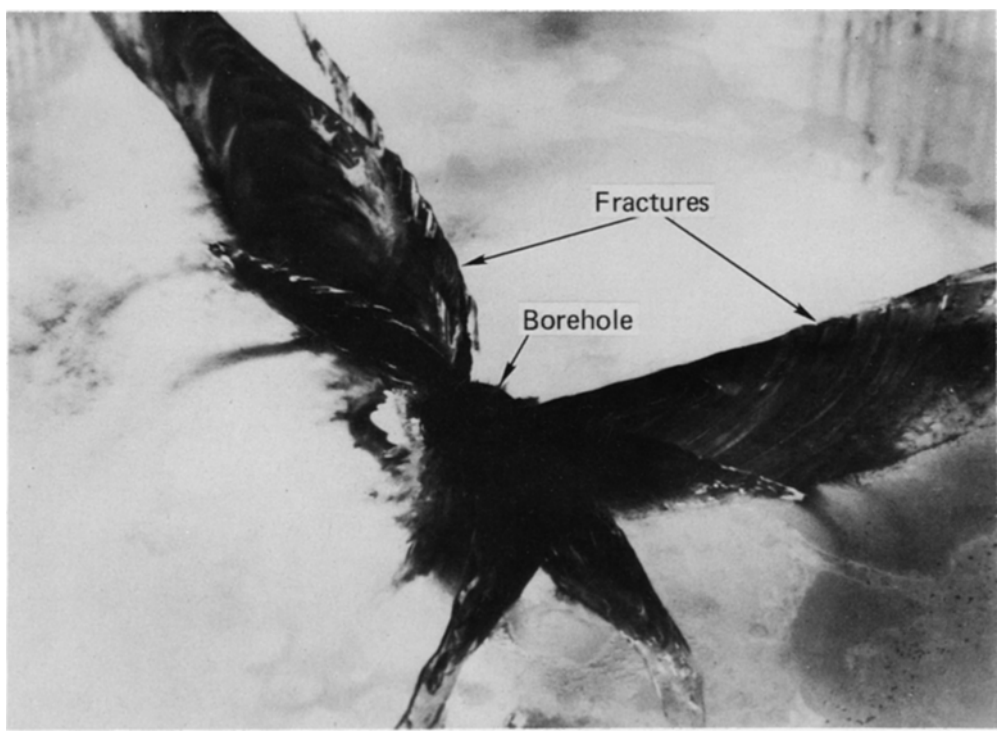


Figure 6. Oblique view showing fractures intersecting midplane of plexiglas block after detonation of explosive – unsheathed borehole.

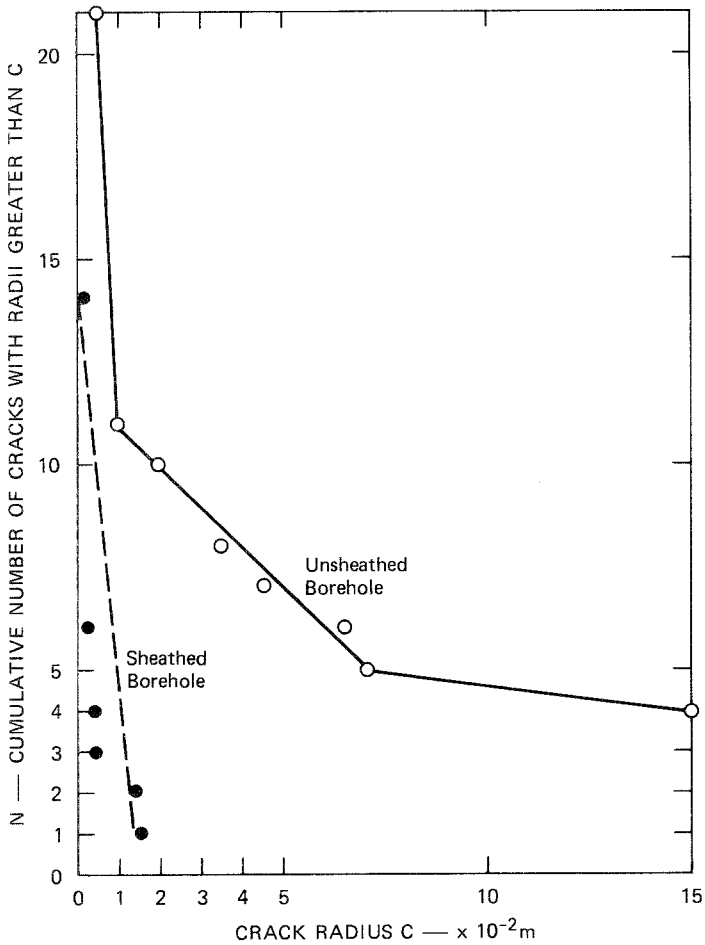


Figure 7. Cumulative crack number *versus* crack radius for both laboratory springing experiments.

## 5. Analysis and conclusions

Some features of the experiments should be noted. First, the calculational simulations of these experiments indicated that radial cracks caused by the circumferential tensile stresses alone would be about 0.02 to 0.05 m long. (At greater distances the circumferential stresses were compressive because of the confining pressure, and thus no cracking was expected.) This prediction is in good agreement with the crack lengths observed in the sheathed borehole experiment (Fig. 7).

Second, the primary effect of the explosive gases is to cause the crack length to increase by a factor of 5 to 10. [A secondary effect is a 50% increase in the number of small (i.e., $< 5 \times 10^{-3}$ m) fractures in the unsheathed borehole experiment compared with the sheathed borehole experiment.]

Third, these results cannot be explained by assuming that the explosive gases are acting quasi-statically to pressurize the borehole and/or cracks. That is, if the gases acted quasi-statically, only one or two cracks would grow in response to the gas penetration because a quasi-static stress field causes the longest crack to extend first, and the least gas pressure to cause crack extension is the pressure required to extend two diametrically opposed radial

cracks [17, 18]. In fact, several cracks grow (Fig. 7), suggesting that a complete analysis must account for dynamic effects.

Fourth, the experiments show that the gases do, in fact, penetrate the cracks and that the gases do reach the crack tips (Fig. 6). The calculations indicate that the gas pressure in the cracks causes the observed increase in crack length seen in Fig. 7. Thus, not only do the gases penetrate the cracks, but the gas pressure in the crack is large enough to extend the cracks. Comparing the crack lengths in the two experiments show that even with the confining pressure the explosive gases increased the crack lengths by a factor of 5 to 10, which is in approximate agreement with the increase in crack length of 3 to 25 predicted by the calculations with confining pressure.

**Acknowledgment**

I wish to thank D. Keough and D. Shockey for reading the first draft of this paper, and D. Curran for many helpful discussions and criticisms of this work.

REFERENCES

[1] S.L. McHugh, P.S. De Carli, and D. Keough, "Small-Scale Field Experiments with An Analysis to Evaluate the Effects of Tailored Pulse Loading on Fracture and Permeability", SRI Annual Report to Department of Energy, Morgantown Energy Technology Center, Morgantown, WV, SRI Project PYU 8621, SRI International Menlo Park (1980).
[2] R.A. Schmidt, N.R. Warpinski, P.W. Cooper, "In Situ Evaluation of Several Tailored-Pulse Well-Shooting Concepts", paper presented at Society of Petroleum Engineers Meeting, Pittsburg, PA (May 1980).
[3] I.N. Sneddon and H.A. Elliott, *Quarterly Applied Mathematics* 4 (1946) 262–267.
[4] O.L. Bowie, *Journal of Mathematics and Physics* 35 (1956) 60–71.
[5] H. Kutter, *International Journal of Fracture Mechanics* 6 (1970) 233–247.
[6] T.P. Bligh, in *Advances in Rock Mechanics*, Proceedings of the Third Congress of the International Society for Rock Mechanics (Denver, CO) Vol. 2, Part B (1974) 1421–1425.
[7] M.P. Hardy, "Fracture Mechanics Applied to Rock," Ph.D. thesis, University of Minnesota (1973).
[8] C.M. Lownds, *Journal of South African Institute of Mining and Metallurgy* 165–180.
[9] R.A. Westmann, *Journal of Mathematics and Physics* 44 (1977) 619–624.
[10] P.S. Theocaris and N.J. Ioakimidis, *Journal of Applied Mechanics* 44 (1977) 619–624.
[11] U. Langefors and B. Kihlstrom, *The Modern Technique of Rock Blasting*, third edition, Halstead Press, John Wiley and Sons (1978).
[12] F. Ouchterlony, in *Proceedings of the Third Congress of the International Society Rock Mechanics* (Denver, CO) (1974) 1377–1383.
[13] L.D. Clark and S.S. Saluja, *Transactions American Institute of Mining Engineers* 229 (1964) 78–90.
[14] S.S. Saluja, in *Status of Practical Rock Mechanics*, Proceedings of the Ninth Symposium on Rock Mechanics (Golden, CO) American Institute of Mining Engineers (1968) 297–319.
[15] C.H. Johansson and P.A. Persson, in *Proceedings of the Third Congress of the International Society for Rock Mechanics* (Denver, CO) (1974) 1557–1566.
[16] F. Ouchterlony, *Engineering Fracture Mechanics* 8 (1976) 447–448.
[17] H.K. Kutter and C. Fairhurst, in *Practical Rock Mechanics*, Proceedings Ninth Symposium on Rock Mechanics (Golden, CO) American Institute of Mining Engineers (1968) 265–284.
[18] D.D. Porter and C. Fairhurst, in *Dynamic Rock Mechanics*, Proceedings of the Twelfth Symposium on Rock Mechanics (Rolla, MO) American Institute of Mining Engineers (1971) 497–515.
[19] N.R. Warpinski, R.A. Schmidt, H.C. Walling, P.W. Cooper and S.J. Finley, "High Energy Gas Frac.," Sandia Report SAND 78-2342, Sandia Laboratories, Albuquerque, NM (December 1978).
[20] J.W. Dally, W.L. Fourney and D.C. Holloway, *International Journal of Rock Mechanics Mining Science and Geomechanics*, Abstract 12 (1975) 5–12.
[21] D.L. Coursen, *Acta Astronautica* 6 (1979) 341–363.
[22] L. Seaman, "A Computational Model for Dynamic Tensile Microfracture with Damage in One Plane," SRI Poulter Laboratory Technical Report 001-80, SRI International, Menlo Park (February 1980).
[23] L. Seaman, and D.R. Curran, "PUFF 8 Computer Program For One-Dimensional Stress Wave Propagation," SRI Final Report to U.S. Army Ballistics Research Laboratory, MD, SRI Project PYU 6802, SRI International, Menlo Park (1978).
[24] S.L. McHugh, W.J. Murri, L. Seaman, D.R. Curran and D.D. Keough, "Fracture of Devonian Shale by

Tailored Pulse Loading," SRI Final Report to Department of Energy, Morgantown Energy Technology Center, Morgantown, WV, SRI Project PYU 6700, SRI International, Menlo Park (December 1978).
[25] S.L. McHugh, "The Effect of Explosive Gases on the Fracture Process in a Geologic Solid," SRI Poulter Laboratory Technical Report 002-79, SRI International, Menlo Park (November 1979).
[26] D.J. Cagliostro, "Experiments on the Response of Hexagonal Subassembly Ducts to Radial Loads," SRI Second Interim Report to Argonne National Laboratory, SRI Project PYD 1960, SRI International, Menlo Park (August 1975).
[27] A.H. Shapiro, *The Dynamics and Thermodynamics of Compressible Fluid Flow*, Volumes I and II, Ronald Press Co., New York (1953).

## Appendix. Crack lengths produced by internally pressurized crack with confining pressure

If the fluid in the cracks is a perfect gas that expands isentropically from the borehole into the cracks [27], then

$$P_i v_i^{\gamma} = P_f v_f^{\gamma}, \tag{A-1}$$

where $P_i$ and $v_i$ are the initial pressure in the borehole and borehole volume, $P_f$ and $v_f$ are the final pressure and volume of the crack and borehole, and $\gamma$ is the ratio of specific heats of the fluid. When the crack stops growing, assuming equilibrium and neglecting borehole expansion,

$$P_i v_i^{\gamma} = P_f (v_c + v_i)^{\gamma}, \tag{A-2}$$

where $P_f$ is the equilibrium pressure in the crack and borehole, and the crack volume, $v_c$ is

$$v_c = 0.5\pi n C^2 w, \tag{A-3}$$

where $n$ is the number of cracks, $C$ is the crack radius, and $w$ is the crack width (assuming half-penny-shaped cracks of constant width).

To relate the stress intensity to the crack volume and pressure in relation (A-1), we used the following procedure. The stress intensity was computed for a single penny-shaped internally pressurized crack and no confining pressure:

$$K_{\mathrm{I}} = \frac{2}{\sqrt{\pi}} P_c \sqrt{C}, \tag{A-4}$$

where $P_c$ is the pressure in the crack [assumed constant so that (A-1) can be used]. A crack is unstable if

$$K_{\mathrm{Ic}} < \frac{2}{\sqrt{\pi}} P_c \sqrt{C} \tag{A-5}$$

and stable if

$$K_{\mathrm{Ic}} > \frac{2}{\sqrt{\pi}} P_c \sqrt{C}. \tag{A-6}$$

Fig. A-1 shows the stability criterion in the form

$$C = \frac{K_{\mathrm{Ic}}^2}{(2/\sqrt{\pi})^2} P_c^{-2}. \tag{A-7}$$

A combination of $C$ and $P_c$ that falls in the region noted as unstable will allow the crack to grow; otherwise, it will not grow.

However, as the crack grows the pressure will decrease as the crack volume increases as

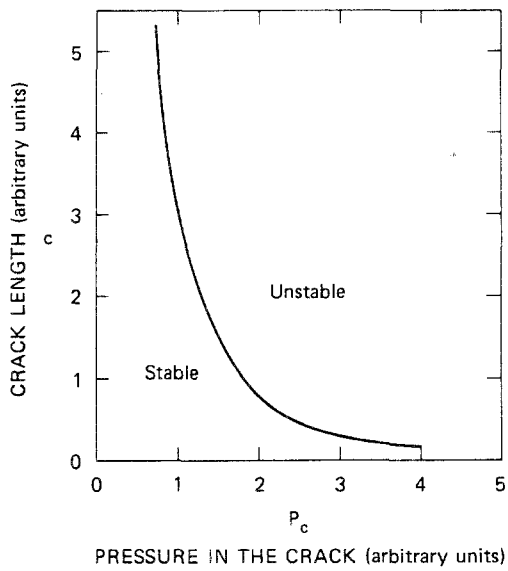


Figure A-1. Crack length *versus* pressure in the crack showing the regions where a crack is stable or unstable.

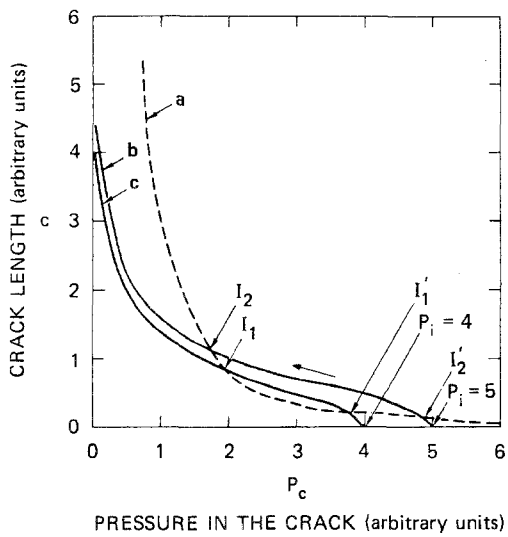


(a) $C = \left(\frac{K_{Ic}^2}{A^2}\right) P_c^{-2}$ and $\frac{K_{Ic}^2}{A^2} = 3$ (Arbitrary)

(b) $C = \left\{\frac{1}{B}\left[\left(\frac{P_i}{P_c}\right)^{1/\gamma} - 1\right]\right\}^{1/2}$ $B = 1, \gamma = 1.3, P_i = 5$

(c) $C = \left\{\frac{1}{B}\left[\left(\frac{P_i}{P_c}\right)^{1/\gamma} - 1\right]\right\}^{1/2}$ $B = 1, \gamma = 1.3, P_i = 4$

Figure A-2. Crack length *versus* pressure in the crack showing the path followed by an expanding crack.

shown by (A-1) through (A-3), and consequently the stress intensity will change. Equations (A-2) and (A-3) also relate $C$ to $P_c$. That is, rewriting (A-2) and setting $P_c = P_f$, we have

$$P_c = P_i\left[\frac{v_i}{v_f}\right]^{\gamma} \tag{A-8}$$

$$= P_i\left[\frac{v_c}{v_i} + 1\right]^{-\gamma} \tag{A-9}$$

$$= P_i(BC^2 + 1)^{-\gamma}, \tag{A-10}$$

where $v_f = v_c + v_i$ and $B = 0.5, n\pi w/v_i = \text{constant}$. Then,

$$C = \left\{B^{-1}\left[\left(\frac{P_i}{P_c}\right)^{1/\gamma} - 1\right]\right\}^{1/2} \tag{A-11}$$

which require $P_c < P_i$, and as $P_i \to P_c$, $C \to 0$ or as $P_c \to 0$, $C \to \infty$. Figure A-2 shows (A-11) plotted with (A-7).

In this example, a crack with initial pressure $P_i = 4$ or 5 (curves *b* or *c* in Fig. A-2) will follow the path indicated by the arrow. It has been assumed that the crack starts growing in response to the tensile stresses (from an explosive detonated in the borehole, for example). Thus the initial intersection points (labeled $I_1'$ and $I_2'$) between the curve for the stress intensity criterion (*a*) and the pressure-volume curves (*b* or *c*) are likely to have been passed during the early stages of crack growth. Consequently, the crack will continue growing until it reaches the second intersection point ($I_1$ or $I_2$). At $I_1$ or $I_2$ the combination of the pressure in the crack and the crack length causes the stress intensity to equal the fracture arrest toughness, $K_{Ia}$, and the crack growth stops. This condition can be expressed by combining (A-1) through (A-4):

$$K_{Ia} = \frac{2}{\sqrt{\pi}} P_i[v_i/(0.5\pi nC^2 w + v_i)]^{\gamma}\sqrt{C} \tag{A-12}$$

$$C^{2-[1/(2\gamma)]} + \left(\frac{2v_i}{n\pi w}\right)C^{-[1/(2\gamma)]} - \left(\frac{2v_i}{n\pi w}\right)\left[\frac{2P_i}{\sqrt{\pi}K_{Ia}}\right]^{1/\gamma} = 0. \tag{A-13}$$

In many cases the middle term of (A-13) is small in comparison to the other terms so that

$$C \sim \left(\frac{2v_i}{n\pi w}\right)^{[2\gamma/(4\gamma-1)]}\left(\frac{2P_i}{\sqrt{\pi}K_{Ia}}\right)^{[1/(2\gamma-0.5)]}. \tag{A-14}$$

Figure A-3 shows (A-14) plotted for a typical borehole shooting experiment [25] and the conditions of 1, 5, or 10 cracks and no confining pressure.

The results shown in Fig. A-3 indicate that even relatively moderate borehole pressures may effectively extend cracks. These final crack lengths are 10 to 100 times larger when the borehole gases pressurize the cracks than when the tensile stresses (Section 1) act alone.

If a confining pressure exists, its effect on crack length can be estimated using this procedure and assuming that the total stress intensity at the crack tip is the result of the internal pressure minus the confining pressure. Equation (A-4) becomes

$$K_I = \frac{2}{\sqrt{\pi}}(P_c - \sigma)\sqrt{C}, \tag{A-15}$$

where $\sigma$ is the confining pressure. Substituting (A-2) and (A-3) into (A-15) we have

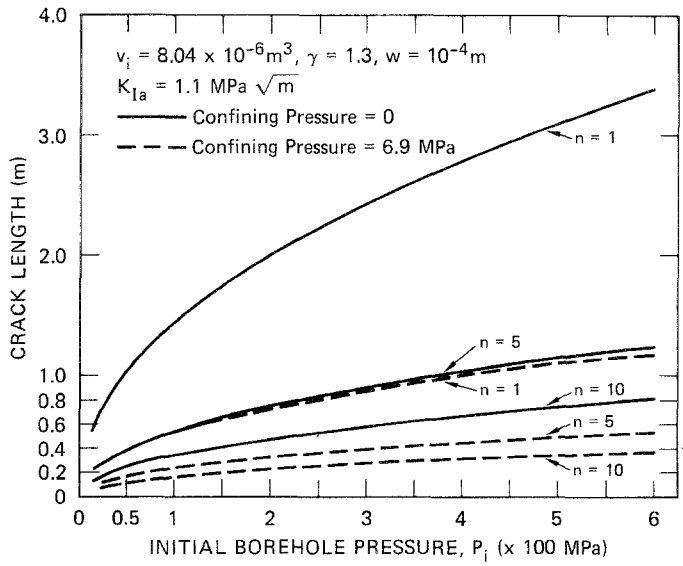


Figure A-3. Crack length as a function of initial borehole pressure. n: number of cracks.

$$\frac{2}{\sqrt{\pi}}\sqrt{C}\left\{P_i\left[\frac{\pi n w}{2v_i}C^2+1\right]^{-\gamma}-\sigma\right\}-K_{Ia}=0, \tag{A-16}$$

where all terms are as previously defined. Equation (A-16) was solved numerically for $C$ at different values of $P_i$ and a confining pressure of 6.9 MPa (1000 psi); the results are shown in Fig. A-3. The primary effect of the 6.9-MPa confining pressure is to reduce the crack lengths by a factor of 2 to 3.

RÉSUMÉ

Une mise en charge explosive dans des configurations d'alésages a été étudiée en vue d'établir l'importance relative de la pression interne de gaz et des tensions circonférentielles induites par l'onde des contraintes pour des fissures radiales en cours d'extension prenant leur origine sur les parois de l'alésage. Des calculs simples d'une fissure en cours d'extension avec ou sans pression de confinement on été effectués en vue d'estimer une frontière supérieure de longueur de fissure qui résulterait seulement de la pression interne, à comparer avec la longueur de fissure qui résulterait seulement des contraintes de traction. Ces calculs ont indiqué que la pression interne de gaz pouvait accroitre la longueur d'une fissure d'un facteur 10 à 100 (sans pression de confinement) ou de 3 à 25 (dans le cas d'une pression de confinement de 6,5 MPa (1000-psi)), lorsqu'on se rapporte à l'action simple des contraintes de traction. Des essais simples de laboratoire ont été effectués en utilisant des charges cylindriques de 3,2 mm 0 sur 152 mm de long disposées dans un alésage de 13 mm 0 foré dans des cylindres de plexiglas transparent de 30 mm 0 sur 30 mm de long, en vue de vérifier les résultats du calcul. Deux essais ont été effectués: l'un recourant à un mince chambrage en acier (1/2 mm) en vue de contenir les gaz de l'explosion et l'autre sans chambrage, de sorte que les gaz de l'explosion pouvaient pénétrer et pressuriser les fissures. Une pression de confinement de 6,9 MPa (1000-psi) a été appliquée aux cylindres de plexiglas dans les deux types d'essai en vue de simuler au mieux les conditions réelles et de contenir les fissures dans le cylindre; toutes les autres conditions d'essai étaient identiques. Ces essais ont indiqué que l'effet principal des gaz résultant de l'explosion était d'accroitre la fissure d'un facteur de 5 à 10, par rapport au cas où les contraintes de traction agissent seules. Ceci est en accord approximatif avec les prédictions.